Silencing lncRNA CDKN2B-AS1 Alleviates Childhood Asthma Progression Through Inhibiting ZFP36 Promoter Methylation and Promoting NR4A1 Expression

Zhixin Chen (zhixinc@21cn.com)
Nanyang Central Hospital https://orcid.org/0000-0001-9222-9037
Nuandong Fan
Nanyang Central Hospital
Guangsheng Shen
Nanyang Central Hospital
Jing Yang
Nanyang Central Hospital

Research Article

Keywords: LncRNA CDKN2B-AS1, childhood asthma, ZFP36, NR4A1, NF-κB signaling pathway.

Posted Date: November 15th, 2021

DOI: https://doi.org/10.21203/rs.3.rs-1037745/v1

Abstract

LncRNA cyclin-dependent kinase inhibitor 2B antisense RNA 1 (CDKN2B-AS1) was found to be upregulated in plasma of patients with bronchial asthma. This study aimed to explore the roles and mechanisms of CDKN2B-AS1 in childhood asthma. We found that CDKN2B-AS1 was upregulated and zinc finger protein 36 (ZFP36) mRNA was downregulated in blood samples of children with asthma compared with healthy controls as measured by RT-qPCR. Human bronchial epithelial cell line BEAS-2B was treated with LPS to induce inflammation model. Small interfering RNA against CDKN2B-AS1 (si-CDKN2B-AS1) was transfected into LPS-treated BEAS-2B cells, and we observed that CDKN2B-AS1 silencing increased cell viability and inhibited apoptosis and inflammation cytokine levels in LPS-treated BEAS-2B cells. Methylation-specific PCR, ChIP and RIP assays indicated that CDKN2B-AS1 inhibited ZFP36 expression by recruiting DNMT1 to promote ZFP36 promoter methylation. Co-IP assay verified the interaction between ZFP36 and nuclear receptor subfamily 4 group A member 1 (NR4A1) proteins. Then rescue experiments revealed that ZFP36 knockdown reversed the effects of CDKN2B-AS1 silencing on BEAS-2B cell functions. ZFP36 overexpression facilitated apoptosis, inflammation and p-p65 expression in BEAS-2B cells, while NR4A1 knockdown reversed these effects. Additionally, CDKN2B-AS1 silencing alleviated airway hyperresponsiveness and inflammation in ovalbumin (OVA)-induced asthma mice. In conclusion, silencing lncRNA CDKN2B-AS1 enhances BEAS-2B cell viability, reduces apoptosis and inflammation *in vitro* and alleviated asthma symptoms in OVA-induced asthma mice *in vivo* through inhibiting ZFP36 promoter methylation and NR4A1-mediated NF-κB signaling pathway.

1 Introduction

Asthma is a common chronic inflammatory airways disease, which is characterized by various typical clinical symptoms, such as coughing, wheezing, chest tightness, shortness of breath and dyspnea [1]. The pathological features of asthma include persistent airway inflammation, inflammatory cell infiltration, and release of pro-inflammatory cytokines and mediators [2]. Asthma usually develops during childhood and severely affects the lung function and quality of life of children. Diagnose and treatment for childhood asthma have always remained a great challenge because of its complex pathogenesis and multiple triggers, such as genetic, epigenetic, developmental, and environmental factors [3]. Although most children with asthma can relieve asthma symptoms and achieve adequate asthma control through avoidance of triggering factors and medication, there is no available complete cure for childhood asthma up to now. Thus, more efforts are urgently required to clarify the molecular mechanism of childhood asthma progression and develop effective therapeutic targets.

Long non-coding RNAs (lncRNAs) are non-coding RNAs with more than 200 nucleotides in length, which have been revealed to play crucial roles in the aberrant regulation and pathogenesis of airway disease. In recent years, a large number of lncRNAs related to the occurrence and development of childhood asthma have been continuously discovered and identified. For instance, lncRNA bromodomain adjacent to zinc finger domain 2B (lnc-BAZ2B) was found to be significantly upregulated in peripheral blood mononuclear cells of children with asthma, and lnc-BAZ2B promoted M2 macrophage activation and inflammation in

children with asthma in a cockroach allergen extract-induced asthma model through stabilizing the pre-mRNA of its cis target gene BAZ2B [4]. A study revealed the pro-inflammatory and pro-fibrotic role of lncRNA RMRP in pediatric asthma through targeting microRNA-206/CCL2 axis [5]. Moreover, current evidence showed that lncRNA CDKN2B-AS1, also known as lncRNA ANRIL, was upregulated in plasma samples of bronchial asthma patients compared with healthy controls, and lncRNA CDKN2B-AS1 is a potentially indicative of disease exacerbation, severity and inflammation for bronchial asthma [6]. More importantly, a recent review has described the role of lncRNA CDKN2B-AS1 and highlighted its potential as a biomarker in various non-cancerous lung diseases [7]. However, whether lncRNA CDKN2B-AS1 is involved in the development of childhood asthma is still poorly understood.

Zinc finger protein 36 (ZFP36), also known as tristetraprolin or TTP, is identified as a prominent inflammatory regulator related to autoimmunity, which may suppress inflammatory response by regulating the mRNA stability of several important inflammatory cytokines [8]. More notably, a previous study analyzed the gene expression profiles in the blood of moderate asthma patients and healthy controls, and identified ZFP36 as one of the optimal asthma biomarkers [9]. Recent evidence demonstrated that ZFP36 expression was downregulated in hepatocellular carcinoma cells by methylation of a specific single CpG site in ZFP36 promoter, indicating that ZFP36 expression is affected by epigenetics modification [10]. Nuclear receptor subfamily 4 group A member 1 (NR4A1), also known as Nur77, is a member of the NR4A subfamily of nuclear hormone receptors, which plays critical roles in inflammatory diseases. More importantly, gene set enrichment analyses and ingenuity pathway analyses identified that NR4A1 was associated with COPD and allergic airway inflammatory disease [11]. Additionally, previous evidence showed that NR4A1 relived ovalbumin (OVA)-induced airway inflammation response in a mouse model of allergic airway disease by counteracting NF-κB signaling in lung epithelial cells [12]. These findings indicated NR4A1 might be an important regulator in asthma.

In this study, we found that lncRNA CDKN2B-AS1 was upregulated in blood samples of children with asthma compared with healthy controls. Then we further explored the role of lncRNA CDKN2B-AS1 in childhood asthma progression *in vivo* and *in vitro.* This study revealed a novel regulatory mechanism among lncRNA CDKN2B-AS1, ZFP36 and NR4A1 in childhood asthma progression.

2 Methods

2.1 Clinical samples

In this study, a total of 30 children with asthma (18 males and 12 females, with an average age of 7.1 ± 3.1 years) and 30 healthy children (20 males and 10 females, with an average age of 7.7 ± 2.8 years) were recruited from Nanyang Central Hospital. Exclusion criteria were children having heart, liver, kidney, malignant hematological diseases, tumors diseases or other lung diseases. Blood samples were collected from children with asthma before treatment and health control during health examination, and plasma were isolated by centrifugation at 1000 g for 15 minutes and then stored at −80°C. This study was

approved by the Ethnic Committee of Nanyang Central Hospital, and informed consent was obtained from each patient involved in this study.

2.2 Animals

Female BALB/c mice (6–8 weeks old, 20 ± 2 g) were obtained from the Laboratory Animal Center of Zhengzhou University. Mice were maintained in sterile cages under standard conditions (12 h light/dark cycle; temperature 22-25°C; humidity, 55-60%) and free access to standard pellet food and water. All animal experiments in this study were approved by the Animal Ethics Committee of Nanyang Central Hospital.

2.3 Cell lines and culture

The human bronchial epithelial cell line BEAS-2B was obtained from ATCC (Manassas, VA, USA). Cells were cultured in Dulbecco's modified Eagle's medium (Gibco, Grand Island, NY) containing 10% fetal bovine serum (FBS; Gibco, Carlsbad, CA), 100 U/mL penicillin and 100 μg /mL streptomycin (Sigma, St. Louis, MO, USA), and maintained with 5% CO_2 at 37°C. When cells were grown to over 80% confluence, 1 μg/mL LPS (Sigma, St. Louis, MO, USA) was added to the BEAS-2B cell medium and incubated for 24 h.

2.4 Cell transfection

Overexpression plasmids of lncRNA CDKN2B-AS1 (pcDNA-CDKN2B-AS1), ZFP36 (pcDNA-ZFP36), small interfering RNAs targeting CDKN2B-AS1 (si-CDKN2B-AS1) and ZFP36 (si-ZFP36), and their corresponding negative controls (vector and scramble) were obtained from RiboBio (Guangzhou, China). Cells were seeded in 6-well plates at a density of 2×10^5 cells/mL, and when reaching 70% confluence, cell transfection were performed by using Lipofectamine™ 2000 (Invitrogen, Carlsbad, CA) according to the manufacturer's instructions. Cells were collected after transfection for 48 h for further experiments.

2.5 RNA extraction and RT-qPCR

The total RNA in plasma were extracted by using QIAamp RNA Blood Mini Kit (Qiagen, Hilden, Germany), and the total RNA of BEAS-2B cells or tissues was extracted by using TRIzol (Invitrogen, Carlsbad, CA) according to the manufacturer's instructions. The cDNA synthesis was performed by using a Prime Script RT reagent Kit (Takara, Dalian, China). RT-qPCR were conducted with SYBR Premix Ex Taq II (Takara, Dalian, China) on an ABI 7500 Real-Time PCR System (Applied Biosystems, Foster City, CA) under the following conditions: 95°C for 1 min, 35 cycles of 95°C for 20 s, 56°C for 10 s and 72°C for 15 s. PCR reaction system contained 12.5 μL of SYBR Premix Ex Taq □, 1.0 μL of RT primer, 1 μL of cDNA sample, and 10.5 μL of double distilled H_2O. Relative gene expression was calculated normalized to glyceraldehyde 3-phosphate dehydrogenase (GAPDH) and calculated by $2^{-\Delta\Delta CT}$ method. Primers were as follows: lncRNA CDKN2B-AS1 (forward: 5'-TGC TCT ATC CGC CAA TCA GG-3', reverse: 5'-GGG CCT CAG TGG CAC ATA CC-3'), GAPDH (forward: 5'-CTG GGC TAC ACT GAG CAC C-3', reverse: 5'-AAG TGG TCG TTG AGG GCA ATG-3').

2.6 CCK-8 assay

Cell viability was measured by using the Cell Counting Kit-8 (CCK-8, Dojindo, Japan) assay. Briefly, after treatment, BEAS-2B cells (1×10^4 cells/well) was seeded into 96-well plates and cultured for 48 h. Then 10 μL of CCK-8 solution was added to wells and incubated for 2 h at 37°C. The absorbance of each well was measured at 450 nm with a Microplate Reader (Bio-Rad, Hercules, CA).

2.4. Cell apoptosis analysis

BEAS-2B cells were collected and stained with the Annexin V-FITC/PI apoptosis detection kit (BD Bioscience, San Jose, CA, USA). Briefly, cells were resuspended in 1× binding buffer (1×10^6 cells/mL). Then 5 μL Annexin V-FITC and 5 μL PI were added into cell suspension and incubated for 15 min in the dark at room temperature. Cell apoptosis was detected by using Flow Cytometer (BD Bioscience, San Jose, CA, USA) according to the manufacturer's instruction.

2.5 Enzyme-linked immunosorbent assay (ELISA)

Following the indicated treatments, the supernatant of BEAS-2B cells or BALF were collected, and then the concentration of inflammatory cytokines including tumor necrosis factor-α (TNF-α), interleukin-1β (IL-1β) and interleukin-6 (IL-6) were determined with the commercial ELISA kits purchased from R&D systems according to the manufacturer’s instructions.

2.6 Western blot analysis

Proteins were extracted from BEAS-2B cells and quantified using the BCA method (Millipore, Billerica, MA, USA). Then equal amount of protein was subjected to 10% SDS-PAGE at 70 V for 30 min then 120 V for 90 min. And the protein bands were transferred to polyvinylidene difluoride (PVDF) membranes (Millipore, Bedford, MA, USA) at 300 mA for 2 h. The membranes were blocked with 5% nonfat milk for 1 h at room temperature and then incubated overnight at 4 ºC with the following primary antibodies obtained from Abcam (Cambridge, UK): rabbit polyclonal anti-ZFP36 antibody (1:1000, ab83579), rabbit polyclonal anti-NR4A1 antibody (1:500, ab13851), rabbit monoclonal anti-p65 antibody (1:1000, ab32536) and rabbit polyclonal anti-GAPDH antibody (1:2500, ab9485), followed by incubation with horseradish peroxidase (HRP)-conjugated goat anti-rabbit IgG (1:2000, ab6721) for 1 h. Subsequently, the protein bands were visualized with ECL detection reagents and analyzed with ImageJ software (National Institutes of Health, Bethesda, MA, USA).

2.7 Methylation-specific PCR (MSP)

MS-PCR was used to detect the methylation status of the ZFP36 promoter. Cell DNA extraction was conducted with the genomic DNA extraction kit (Tiangen Biochemistry Technology Co., Ltd., Beijing, China) according to the manufacturer’s instructions. The DNA concentration was determined using a UV spectrophotometer. The extracted DNA (10 μg) was added with 5.5 μL of 3 mol/L NaOH to denature at 37°C for 10 min. Next, DNA was added with 20 μL of 10 mM hydroquinone and 520 μL of 40.5% sodium hydrogen sulfite, and then covered by 200 μL mineral oil. Then the modified DNA was purified by wizard DNA column. The purified solution was added with 5.5 μL of 3 mol/L NaOH to denature for 10 min, and then 5.5 μL of 3 M sodium acetate and 120 μL cold absolute ethanol were added to precipitate and

recycle DNA. MS-PCR reaction was conducted using ABI7500 quantitative PCR instrument (ABI Company, Oyster Bay, NY). The reaction products were then analyzed by agarose gel electrophoresis and imaged with a gel electrophoresis imaging analysis system.

2.8 Chromatin immunoprecipitation (ChIP)

EZ-Magna ChIP TMA kit (Millipore, Billerica, MA) were employed for chromatin immunoprecipitation (ChIP) analysis following the manufacturer's guideline. Briefly, BEAS-2B cells were cross-linked with 1% formaldehyde for 10 min, and then 125 mM glycine was added to terminate the crosslinking. Next, cells were lysed in lysis buffer, and chromatin fragments at 200-1000 bp were obtained by cracking the cells through ultrasound. The supernatant was centrifuged and the fragments were collected in three tubes, which were supplemented with the target protein specific antibody (DNMT1, ab13537, Abcam) or the negative control antibody (IgG, ab10948, Abcam) for incubation at 4°C overnight. The DNA-protein complex was precipitated with Protein Agarose/Sepharose. The precipitated DNA fragments were purified and subjected to RT-qPCR analysis.

2.9 RNA immunoprecipitation (RIP) assay

The binding of lncRNA CDKN2B-AS1 with DNMT1 was determined by using the Magna RIP RNA-Binding Protein Immunoprecipitation kits (Merck Millipore, Billerica, MA). Briefly, cells were lysed by using a RIPA lysate buffer (Beyotime Biotechnology Co., Shanghai, China) for 5 min, and the supernatant was collected by centrifugation at 4°C. Subsequently, 50 μL of protein A/G-beads was resuspended with 100 μL of RIP wash buffer, and 5 μg of anti-DNMT1 antibody (ab13537, 1:100, Abcam) or NC antibody (IgG, ab10948, 1:100, Abcam) were added and incubated for 30 min at the room temprature. After washed, the protein A/G-bead-antibody complexes were resuspended with 900 μL of RIP wash buffer and incubated with 100 μL of supernatant overnight at 4°C. After immunoprecipitation, the protein A/G-beads were collected and washed with RIP wash buffer and deposited 5 times. Finally, the protein A/G-bead-protein complexes were blended with proteinase K to extract RNA. Relative RNA expression was analyzed with RT-qPCR.

2.10 Co-immunoprecipitation (Co-IP) assay

BEAS-2B cells were lysed RIPA buffer (Beyotime, Shanghai, China), and the supernatant was collected and incubated with ZFP36 antibody at 4°C overnight. Then the mixture was incubated with 100 μL of protein A/G agarose beads (Takara Biotechnology, Dalian, China) overnight at 4℃. Subsequently, the agarose beads-antigen-antibody complex was collected by instantaneous centrifugation and washed with PBS for three times. Next, the complex was boiled with protein loading buffer for 5 min. The supernatant was collected by centrifugation and analyzed by using Western blot to detect the expression of interaction proteins.

2.11 Animal experimental protocols

BALB/c mice were randomly divided into three groups (n=8 per group): control group, OVA group, and OVA+si-CDKN2B-AS1 group. On day 1 and 14, the mice were sensitized with 20 μg of ovalbumin (OVA) with 2 mg aluminum hydroxide adsorbed in 200 μL of PBS by intraperitoneal injection. From day 21 to

23, mice were challenged by intranasal inhalations of 100 μg OVA adsorbed in 20 μL of PBS once a day. For si-CDKN2B-AS1 treatment, 100 μg of si-CDKN2B-AS1 was administered daily via intraperitoneal injection on day 21 to 23. For NC group, mice were treated with an equal volume of PBS by using the same method. The mice were euthanized 24 h after the last challenge.

2.12 Measurement of Airway Hyperresponsiveness

Airway hyperresponsiveness (AHR) was detected by using noninvasive whole-body plethysmography (Model PLY 3211; Buxco, Sharon, CT, USA). Within 24 h following the final OVA challenge, the mice in all groups were treated with 0, 5, 10, 25 and 50 mg/mL methacholine aerosol for 3 min, followed by 2 min of rest, and the enhanced pause (Penh) value of unrestrained mice within 5 min was recorded.

2.13 Collection of bronchoalveolar lavage fluid (BALF) and cell counting

After mice were anesthetized, the tracheas were cannulated and lavaged with 0.8 mL aliquots of cold PBS twice to collect bronchoalveolar lavage fluid (BALF). The BALF samples were immediately centrifuged and kept at -80℃. The cell pellets from BALF were resuspended in PBS (0.5 mL). Total cell counting was done with a hemocytometer. And the Kwik-Diff staining set (Thermo, USA) was used for counting of differential cell counts (eosinophils, macrophages, neutrophils, and lymphocytes) in BALF according to the manufacturer's instructions.

2.14 Histopathological analysis

Lung tissues were collected and fixed in 10 % neutral buffered formalin, and then embedded in paraffin and sliced. Paraffin sections were stained with hematoxylin and eosin (H&E) using a standard protocol and analyzed by light microscopy.

2.15 Measurement of the level of OVA-specific IgE in serum

On day 24 after the last OVA challenge, mice were euthanized and the blood samples were collected by puncturing the vena cava. The blood samples were centrifuged at 1000 g for 10 min to obtain serum samples. The level of OVA-Specific immunoglobulin E (IgE) in serum was measured by ELISA kit (Abcam, Cambridge, UK) according to the manufacturer's instructions.

2.16 Statistical analysis

Data analysis was performed by SPSS version 22.0 software. Experimental results from three times independent experiments were presented as mean± standard deviation (SD). Comparisons between two groups or multiple groups were performed by using student's t-test or analysis of variance (ANOVA), respectively. $P<0.05$ was considered to be statistically significant.

3 Results

3.1 LncRNA CDKN2B-AS1 was upregulated and ZFP36 was downregulated in children with asthma.

To investigate whether CDKN2B-AS1 is involved in childhood asthma progression, we firstly detected the expression of CDKN2B-AS1 in children with asthma and healthy controls by using RT-qPCR. As shown in Fig. 1A, CDKN2B-AS1 was upregulated in blood samples of children with asthma compared with that in healthy controls. Moreover, we also found that the expression of ZFP36 mRNA was downregulated (Fig. 1B). Interestingly, we further found that CDKN2B-AS1 expression was negatively correlated with ZFP36 expression (Fig. 1C), which may imply a potential regulatory relationship between CDKN2B-AS1 and ZFP36 in the development of childhood asthma.

3.2 Silencing CDKN2B-AS1 promoted BEAS-2B cell viability, and inhibited apoptosis and inflammation

To further explore the roles of CDKN2B-AS1 in childhood asthma progression, BEAS-2B cells were treated with LPS to induce inflammation model, and then si-CDKN2B-AS1 was transfected into BEAS-2B cells. RT-qPCR results showed that CDKN2B-AS1 expression was upregulated in LPS-treated BEAS-2B cells, while transfection of si-CDKN2B-AS1 decreased CDKN2B-AS1 expression. CCK-8 assay showed that BEAS-2B cell viability was inhibited by LPS treatment, but promoted by silencing CDKN2B-AS1 (Fig. 2B). Then we found that LPS treatment promoted BEAS-2B cell apoptosis, while silencing CDKN2B-AS1 inhibited LPS-induced cell apoptosis (Fig. 2C). Moreover, LPS treatment promoted the secretion of inflammatory cytokines including TNF-α, IL-1β and IL-6 in BEAS-2B cells, while silencing CDKN2B-AS1 inhibited the secretion of inflammatory cytokines (Fig. 2D-2F). All results indicated that silencing CDKN2B-AS1 promotes BEAS-2B cell viability, and inhibits apoptosis and inflammation.

3.3 CDKN2B-AS1 reduced ZFP36 expression by promoting ZFP36 promoter methylation

To investigate the regulatory relationship and mechanism between CDKN2B-AS1 and ZFP36, we first transfected pcDNA-CDKN2B-AS1 or si-CDKN2B-AS1 into BEAS-2B cells, the transfection efficiency of pcDNA-CDKN2B-AS1 and si-CDKN2B-AS1 were shown in Fig. 3A. Moreover, Western blotting displayed that transfection of pcDNA-CDKN2B-AS1 significantly decreased ZFP36 expression, while transfection of si-circ_0001756 increased ZFP36 expression in BEAS-2B cells, (Fig. 3B). Subsequently, CpG islands in ZFP36 promoter region were analyzed using a 3000-bp fragment in the ZFP36 promoter region via the MethPrimer (http://www.urogene.org/cgi-bin/methprimer/methprimer.cgi) website. The data indicated that the CpG islands existed in the ZFP36 promoter region (Fig. 3C), suggesting that the expression of ZFP36 was influenced by promoter methylation. MS-PCR was further performed to investigate the methylation of ZFP36 promoter in BEAS-2B cells after transfection. As presented in Fig. 3D, ZFP36 methylation was enhanced following CDKN2B-AS1 overexpression and reduced following CDKN2B-AS1 silencing in BEAS-2B cells, and ZFP36 methylation was inhibited by addition of DNA methyltransferase

inhibitor (5-Aza-CdR), but rescued after CDKN2B-AS1 overexpression. Furthermore, ChIP results showed that DNA methyltransferase 1 (DNMT1) was enriched in the promoter region of ZFP36, and CDKN2B-AS1 overexpression promoted the enrichment of DNMT1 in ZFP36 promoter (Fig. 3E). RIP assay further illustrated that compared with IgG treatment, DNMT1 significantly increased the enrichment of CDKN2B-AS1 (Fig. 3F). Collectively, the obtained results demonstrated that CDKN2B-AS1 reduced ZFP36 expression by promoting ZFP36 methylation.

3.4 CDKN2B-AS1 regulated BEAS-2B cell viability, apoptosis and inflammatory response by inhibiting ZFP36 expression

To explore whether CDKN2B-AS1 exerted its functions in childhood asthma progression by regulating ZFP36 expression, si-CDKN2B-AS1 were transfected into LPS-treated BEAS-2B cells alone or together with si-ZFP36. Western blotting indicated that LPS treatment reduced ZFP36 expression, and transfection of si-CDKN2B-AS1 increased ZFP36 expression in LPS-treated BEAS-2B cells, while transfection of si-ZFP36 reversed this effect (Fig. 4A). Moreover, CCK-8 assay showed that BEAS-2B cell viability was suppressed by LPS treatment, silencing CDKN2B-AS1 increased LPS-treated BEAS-2B cell viability, which were then reversed by transfection of si-ZFP36 (Fig. 4B). In addition, flow cytometry and ELISA results showed that silencing CDKN2B-AS1 attenuated BEAS-2B cell apoptosis (Fig. 4C) and the secretion of TNF-α IL-1β and IL-6 (Fig. 4D-4F) promoted by LPS treatment, while transfection of si-ZFP36 reversed these effects. These results revealed that CDKN2B-AS1 regulates BEAS-2B cell viability, apoptosis and inflammatory response by negatively regulating ZFP36 expression.

3.5 ZFP36 interacts with NR4A1 and positively regulates NR4A1 expression

The potential interacting proteins of ZFP36 were predicted with the Genemania tool (http://genemania.org/), which showed that there was a potential interaction between ZFP36 and NR4A1 (Fig. 5A). Subsequently, Co-IP assay verified that both ZFP36 and NR4A1 proteins could be detected by immunoprecipitation with ZFP36 antibody but not with IgG in BEAS-2B cells (Fig. 5B). Moreover, we found that ZFP36 overexpression significantly increased NR4A1 expression, while ZFP36 knockdown decreased NR4A1 expression in BEAS-2B cells (Fig. 5C). Besides, Western blotting further showed that CDKN2B-AS1 overexpression decreased NR4A1 expression, while CDKN2B-AS1 knockdown increased NR4A1 expression in BEAS-2B cells (Fig. 5D).

3.6 ZFP36 regulated BEAS-2B cell viability, apoptosis and inflammatory response by blocking NR4A1-mediated NF-κB signaling pathway

To further investigate whether the effects of ZFP36 and NR4A1 was involved in childhood asthma progression, pcDNA-ZFP36 were transfected into LPS-treated BEAS-2B cells alone or together with si-

NR4A1. Western blotting results showed that LPS treatment repressed NR4A1 expression, and ZFP36 overexpression increased NR4A1 expression, while transfection of si-NR4A1 decreased NR4A1 expression in BEAS-2B cells (Fig. 6A). Moreover, CCK-8 assay showed that BEAS-2B cell viability was inhibited by LPS treatment, ZFP36 overexpression increased LPS-induced BEAS-2B cell viability, which were then reversed by transfection of si-NR4A1 (Fig. 6B). In addition, flow cytometry and ELISA results showed that ZFP36 overexpression suppressed BEAS-2B cell apoptosis (Fig. 4C) and the secretion of TNF-α, IL-1β and IL-6 (Fig. 6D-6F) promoted by LPS treatment, while transfection of si-NR4A1 reversed these effects. Besides, we further found that LPS treatment increased p-p65 expression, and ZFP36 overexpression reduced p-p65 expression, while transfection of si-NR4A1 reversed the inhibited effect of ZFP36 overexpression on NF-κB p65 expression in BEAS-2B cells (Fig. 6G). These results demonstrated that ZFP36 regulates BEAS-2B cell viability, apoptosis and inflammation by promoting NR4A1 expression and blocking NF-κB signaling pathway.

3.7 Silencing CDKN2B-AS1 alleviated asthma symptoms in OVA-induced asthma mice

To further investigate the role of CDKN2B-AS1 in asthma progression *in vivo*, OVA-induced asthma mice model was constructed and si-CDKN2B-AS1 was intraperitoneally injected for treatment. We confirmed the increased CDKN2B-AS1 expression and decreased IGF2BP2 and RAB5A expression in lung tissues of OVA group, and this expression pattern was reversed by si-CDKN2B-AS1 treatment (Fig. 7A-7B). Moreover, the airway hyperresponsiveness of mice was detected through measuring the Penh value. It was showed that mice in all groups showed increased airway hyperresponsiveness as the increased concentration of methacholine, and the Penh value of OVA-induced mice was higher than the control group, while treatment of si-CDKN2B-AS1 significantly reduced the Penh value in OVA-induced mice (Fig. 7C). In histological evaluation, lung samples in control group mice revealed normal lung structure without the obvious inflammatory infiltration. However, the mice in the OVA group displayed infiltration of inflammatory cells into the lung interstitium and alveolar spaces, thick-ening of alveolar walls, and intra-alveolar exudation, while si-CDKN2B-AS1 treatment inhibited OVA-induced inflammatory cell infiltration and thick-ening of alveolar walls (Fig. 7D). Additionally, the infiltration of inflammatory cells (neutrophils, eosinophils, macrophages, and lymphocytes) in BALF was increased significantly in OVA-induced mice, while treatment of si-CDKN2B-AS1 inhibited OVA-induced inflammatory cell infiltration in BALF (Fig. 7E). And ELISA results showed that OVA-specific IgE level (Fig. 7F) in serum and inflammatory cytokines including TNF-α, IL-1β and IL-6 levels (Fig. 7G) in lung tissues were significantly increased in OVA-induced mice, while si-CDKN2B-AS1 treatment significantly inhibited OVA-induced serum IgE level and inflammatory cytokine levels.

4 Discussion

In recent years, increasing evidence has revealed that the altered expression of lncRNAs affects inflammatory response, immune response and lung function and may be used for the development of

specific biomarkers for airway disease [13, 14]. It was previously reported that interleukin-13 treatment increased CDKN2B-AS1 expression in human nasal epithelial cells (HNECs), and knockdown of CDKN2B-AS1 may suppress the production of inflammatory cytokines and mucin in IL-13-treated HNECs via regulation of the miR-15a-5p/JAK2 axis [15]. Furthermore, CDKN2B-AS1 was found to be upregulated in plasma samples of bronchial asthma patients compared with healthy controls, and the expression of CDKN2B-AS1 was positively correlated with pro-inflammatory cytokines secretion exacerbation severity in bronchial asthma patients [6]. Given the role of CDKN2B-AS1 in bronchial asthma, we further explored its underlying role in childhood asthma progression. In the present study, we found that CDKN2B-AS1 was upregulated in blood samples of children with asthma compared with healthy controls. Moreover, silencing CDKN2B-AS1 significantly promotes BEAS-2B cell viability and inhibits apoptosis and inflammatory cytokines secretion *in vitro*, and alleviated airway inflammation and asthma symptoms of OVA-induced asthma mice *in vivo*. In addition, a recent study has implicated that CDKN2B-AS1 negatively regulated A disintegrin and metalloprotease 10 (ADAM10) expression via recruiting DNMT1 to promote ADAM10 DNA methylation, consequently preventing inflammatory response of atherosclerosis [16]. Therefore, CDKN2B-AS1 may regulates the expression of its downstream target genes by promoting DNMT1-mediated DNA methylation. Interesting, our study found that CDKN2B-AS1 negatively regulated ZFP36 expression in BEAS-2B cells by recruiting DNMT1 to promote ZFP36 promoter methylation, thereby modulating cell viability, apoptosis and inflammatory response in BEAS-2B cells.

ZFP36 has been well-studied in inflammatory disorders and plays an important role in inducing the mRNA decay of inflammatory cytokines such as TNF-α, IL-3 and IL-8 [17]. It was found that carbon monoxide-induced ZFP36 mediates the protective effect of carbon monoxide against LPS-induced acute lung injury by enhancing the mRNA decay of proinflammatory cytokines [18]. Moreover, enhancing ZFP36 activity reduced the levels of cytokines, pulmonary inflammation and improved lung function in the cigarette smoke-induced experimental chronic obstructive pulmonary disease (COPD) mice model [19]. In this study, we demonstrated that ZFP36 served as anti-inflammatory gene in LPS-treated BEAS-2B cells, and knockdown of ZFP361 repressed BEAS-2B cell viability and promoted apoptosis and inflammatory response. Besides, available studies have indicated that regulation of ZFP36 expression is affected by epigenetics modification of DNA methylation. For instance, resveratrol showed anticancer activity through suppressing the expression of DNMT1 and inducing demethylation of the ZFP36 promoter in non-small cell lung cancer cells [20]. Additionally, treatment with DNA methylation inhibitor (5-aza dC) increased ZFP36 expression in several HCC cell lines [21]. Similarly, our study implicated that ZFP36 expression was regulated by CDKN2B-AS1-mediated methylation in BEAS-2B cells.

NR4A1 is a key negative regulator of inflammatory responses. Accumulating evidence has suggested that NR4A1 is implicated in the regulation of inflammation and immunity disease [22, 23]. In particular, NR4A1 has been shown to have a protective function in lung inflammation and diseases. For instance, the anti-inflammatory properties and protective effect of NR4A1 on acute respiratory distress syndrome was reported in a study, which indicated that NR4A1 decreased endothelin-1 expression by inhibiting NF-κB and p38 MAPK in LPS-stimulated A549 cells *in vitro*, and NR4A1 reduced endothelin-1 expression and lung injury in LPS-induced ARDS rats [24]. Moreover, emerging evidence has showed that NR4A1

decreased inflammatory cytokines secretion by inhibiting NF-κB signaling in lung epithelial cells, and in OVA-induced allergic airway inflammation mice model, NR4A1 knockout mice show significantly enhanced inflammatory infiltration and mucus secretion [12]. In the present study, we verified the interaction between ZFP36 and NR4A1 in BEAS-2B cells, and revealed that ZFP36 suppressed cell apoptosis and inflammatory cytokines secretion in LPS-treated BEAS-2B cells, while NR4A1 knockdown could reverse these effects. More notably, NR4A1 has been identified as a negative regulator of the NF-κB signaling. NR4A1 was found to regulate cerebral ischemia-induced brain injury through direct interaction with the p65 component of NF-κB and inhibiting the NF-κB signaling pathway [25]. Furthermore, it was reported that NR4A1 suppressed inflammatory response related lung diseases by inhibiting NF-κB signaling both *in vitro* and *in vivo* [26]. Similarly, our findings showed that NR4A1 played an anti-inflammatory role in LPS-treated BEAS-2B cells through blocking the NF-κB signaling pathway.

Taken together, our findings suggested that CDKN2B-AS1 was upregulated in children with asthma compared with healthy controls. Moreover, silencing CDKN2B-AS1 significantly promotes BEAS-2B cell viability and inhibits apoptosis and inflammatory cytokines secretion *in vitro*, and alleviated airway inflammation and asthma symptoms of OVA-induced asthma mice *in vivo*. Mechanistically, CDKN2B-AS1 plays a role in childhood asthma via regulating ZFP36/NR4A1 axis and NF-κB signaling pathway by recruiting DNMT1 to promote ZFP36 promoter methylation. Our study may provide a novel regulatory mechanism and potential therapeutic target for the treatment of childhood asthma.

Declarations

Statements and Declarations

Ethical Approval

This study was approved by the Ethnic Committee of Nanyang Central Hospital, and all subjects had read and signed the informed consent. All animal care and experimental procedures in this study were approved by Animal Care and Use Committee of Nanyang Central Hospital.

Consent for publication

The authors grant their consent to publish the material presented herein.

Availability of data and materials

The data that support the findings of this study are available from the corresponding author upon reasonable request.

Competing Interests

No conflict of interest exits in the submission of this manuscript.

Founding

No applicable.

Authors' contributions

Zhixin Chen designed the experiments. Zhixin Chen, Nuandong Fan, and Guangsheng Shen performed the experimental work. Jing Yang provided statistical analysis as well as figures for the manuscript. Zhixin Chen wrote the manuscript. All authors read and approved the final manuscript.

Acknowledgements

No applicable.

References

1. Buelo, A., S. McLean, and S. Julious, et al. 2018. At-risk children with asthma (ARC): a systematic review. *Thorax* 73 (9): 813–824.
2. Barnig, C., N. Frossard, and B. D. Levy. 2018. Towards targeting resolution pathways of airway inflammation in asthma. *Pharmacol Ther* 186: 98–113.
3. Lebold, K. M., D. B. Jacoby, and M. G. Drake. 2020. Inflammatory mechanisms linking maternal and childhood asthma. *J Leukoc Biol* 108 (1): 113–121.
4. Xia, L., X. Wang, and L. Liu, et al. 2020. lnc-BAZ2B promotes M2 macrophage activation and inflammation in children with asthma through stabilizing BAZ2B pre-mRNA. *J Allergy Clin Immunol*.
5. Yin, H., M. H. Liu, and F. Gao, et al. 2021. Pro-inflammatory and pro-fibrotic role of long non-coding RNA RMRP in pediatric asthma through targeting microRNA-206/CCL2 axis. *J Biol Regul Homeost Agents* 35 (1): 71–83.
6. Ye, S., S. Zhu, and L. Feng. 2020. LncRNA ANRIL/miR-125a axis exhibits potential as a biomarker for disease exacerbation, severity, and inflammation in bronchial asthma. *J Clin Lab Anal* 34 (3): e23092.
7. Poulet, C., M. S. Njock, and C. Moermans, et al. 2020. Exosomal Long Non-Coding RNAs in Lung Diseases. *Int J Mol Sci* 21(10).
8. Fu, M., and P. J. Blackshear. 2017. RNA-binding proteins in immune regulation: a focus on CCCH zinc finger proteins. *Nat Rev Immunol* 17 (2): 130–143.
9. Wang, S. B., and T. Huang. 2019. The early detection of asthma based on blood gene expression. *Mol Biol Rep* 46 (1): 217–223.
10. Sohn, B. H., I. Y. Park, and J. J. Lee, et al. 2010. Functional switching of TGF-beta1 signaling in liver cancer via epigenetic modulation of a single CpG site in TTP promoter. *Gastroenterology* 138 (5): 1898–1908.
11. Hamers, A. A., C. Argmann, and P. D. Moerland, et al. 2016. Nur77-deficiency in bone marrow-derived macrophages modulates inflammatory responses, extracellular matrix homeostasis, phagocytosis and tolerance. *BMC genomics* 17: 162.

12. Kurakula, K., M. Vos, and A. Logiantara, et al. 2015. Nuclear Receptor Nur77 Attenuates Airway Inflammation in Mice by Suppressing NF-κB Activity in Lung Epithelial Cells. *J Immunol* 195 (4): 1388–1398.
13. Zheng, P., C. Huang, and D. Leng, et al. 2020. Transcriptome analysis of peripheral whole blood identifies crucial lncRNAs implicated in childhood asthma. *BMC Med Genomics* 13 (1): 136.
14. Qiu, Y. Y., Y. Wu, and M. J. Lin, et al. 2019. LncRNA-MEG3 functions as a competing endogenous RNA to regulate Treg/Th17 balance in patients with asthma by targeting microRNA-17/ RORγt. *Biomed Pharmacother* 111: 386–394.
15. Liu, H. W., Z. L. Hu, and H. Li, et al. 2021. Knockdown of lncRNA ANRIL suppresses the production of inflammatory cytokines and mucin 5AC in nasal epithelial cells via the miR-15a-5p/JAK2 axis. *Mol Med Rep* 23(2).
16. Li, H., S. Han, and Q. Sun, et al. 2019. Long non-coding RNA CDKN2B-AS1 reduces inflammatory response and promotes cholesterol efflux in atherosclerosis by inhibiting ADAM10 expression. *Aging (Albany NY)* 11 (6): 1695–1715.
17. Yang, C., S. Huang, and X. Wang, et al. 2015. Emerging Roles of CCCH-Type Zinc Finger Proteins in Destabilizing mRNA Encoding Inflammatory Factors and Regulating Immune Responses. *Crit Rev Eukaryot Gene Expr* 25 (1): 77–89.
18. Joe, Y., S. K. Kim, and Y. Chen, et al. 2015. Tristetraprolin mediates anti-inflammatory effects of carbon monoxide on lipopolysaccharide-induced acute lung injury. *Am J Pathol* 185 (11): 2867–2874.
19. Nair, P. M., M. R. Starkey, and T. J. Haw, et al. 2019. Enhancing tristetraprolin activity reduces the severity of cigarette smoke-induced experimental chronic obstructive pulmonary disease. *Clin Transl Immunology* 8 (10): e01084.
20. Fudhaili, A., N. A. Yoon, and S. Kang, et al. 2019. Resveratrol epigenetically regulates the expression of zinc finger protein 36 in non–small cell lung cancer cell lines. *Oncol Rep* 41 (2): 1377–1386.
21. Tran, D. D. H., A. Koch, and A. Allister, et al. 2016. Treatment with MAPKAP2 (MK2) inhibitor and DNA methylation inhibitor, 5-aza dC, synergistically triggers apoptosis in hepatocellular carcinoma (HCC) via tristetraprolin (TTP). *Cell Signal* 28 (12): 1872–1880.
22. Xiong, Y., J. Ran, and L. Xu, et al. 2020. Reactivation of NR4A1 Restrains Chondrocyte Inflammation and Ameliorates Osteoarthritis in Rats. *Front Cell Dev Biol* 8: 158.
23. Nus, M., G. Basatemur, and M. Galan, et al. 2020. NR4A1 Deletion in Marginal Zone B Cells Exacerbates Atherosclerosis in Mice-Brief Report. *Arterioscler Thromb Vasc Biol* 40 (11): 2598–2604.
24. Jiang, Y., Y. Zeng, and X. Huang, et al. 2016. Nur77 attenuates endothelin-1 expression via downregulation of NF-κB and p38 MAPK in A549 cells and in an ARDS rat model. *Am J Physiol Lung Cell Mol Physiol* 311 (6): L1023–Ll1035.
25. Zhang, Y. J., J. R. Song, and M. J. Zhao. 2019. NR4A1 regulates cerebral ischemia-induced brain injury by regulating neuroinflammation through interaction with NF-κB/p65. *Biochem Biophys Res Commun* 518 (1): 59–65.

26. Banno, A., S. P. Lakshmi, and A. T. Reddy, et al. 2019. Key Functions and Therapeutic Prospects of Nur77 in Inflammation Related Lung Diseases. *Am J Pathol* 189 (3): 482–491.

Figures

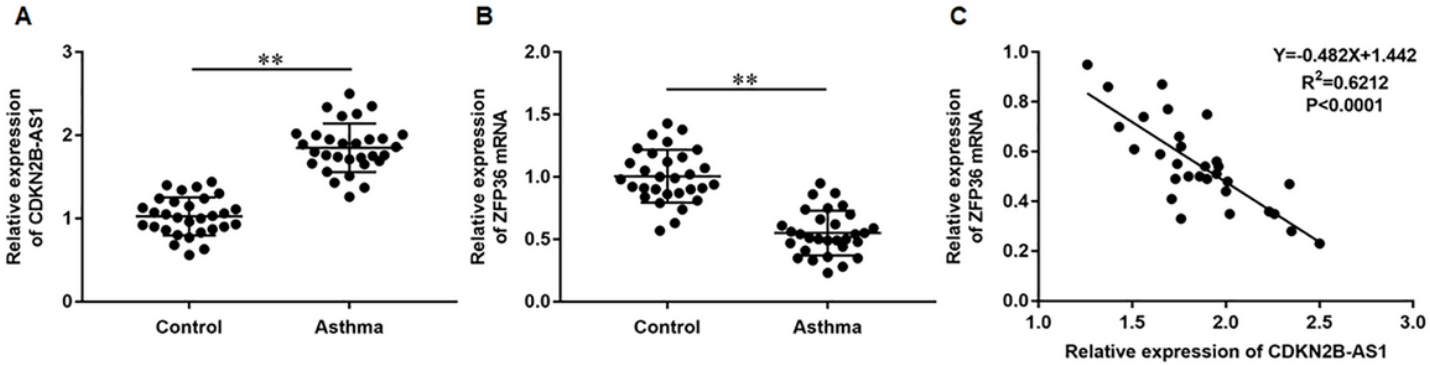

Figure 1

LncRNA CDKN2B-AS1 is upregulated and ZFP36 is downregulated in children with asthma. a total of 30 children with asthma (18 males and 12 females, with an average age of 7.1 ± 3.1 years) and 30 healthy children (20 males and 10 females, with an average age of 7.7 ± 2.8 years) were recruited in this study. RT-qPCR was performed to detected the expression of CDKN2B-AS1 (A) and ZFP36 mRNA (B) in blood samples of children with asthma and healthy controls. (C) CDKN2B-AS1 expression was negatively correlated with ZFP36 expression in children with asthma. Data were presented as mean ± SD. **P<0.01.

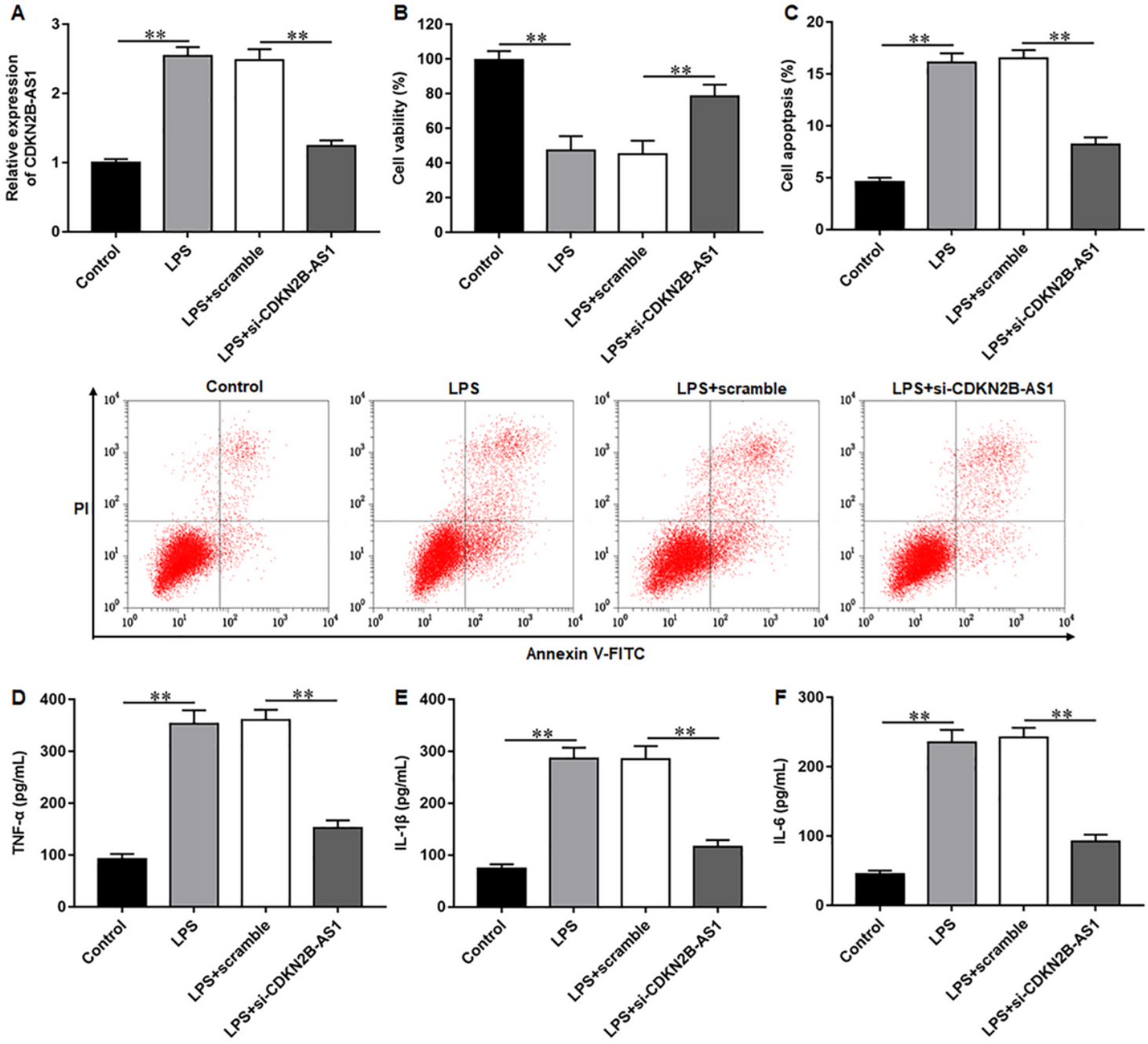

Figure 2

CDKN2B-AS1 regulates BEAS-2B cell viability, apoptosis and inflammatory cytokine secretion. BEAS-2B cells were treated with LPS to induce inflammatory injury model, si-CDKN2B-AS1 and its negative control were transfected into BEAS-2B cells, respectively. (A) RT-qPCR was performed to evaluate the expression of CDKN2B-AS1. (B) BEAS-2B cell viability was measured by using CCK-8 assay. (C) BEAS-2B cell apoptosis was measured by using flow cytometry. (D-F) The levels of TNF-α, IL-1β and IL-6 in cell culture supernatant were detected with ELISA kits. Data were presented as mean ± SD. **P<0.01.

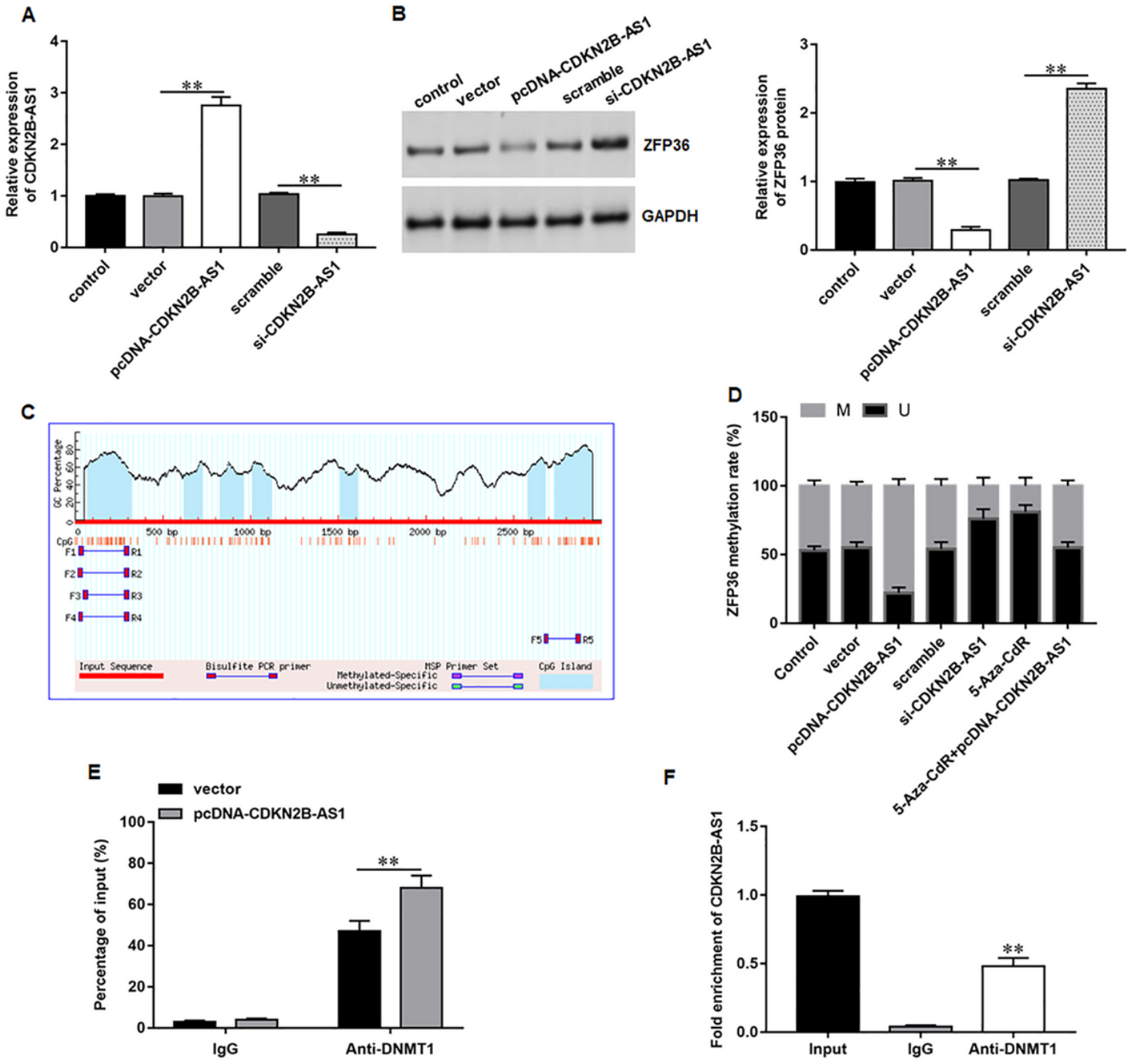

Figure 3

CDKN2B-AS1 promotes ZFP36 promoter methylation by recruiting DNMT1. BEAS-2B cells were transfected with pcDNA-CDKN2B-AS1, si-CDKN2B-AS1 and their corresponding negative controls, respectively. (A) The transfection efficiency of pcDNA-CDKN2B-AS1 and si-CDKN2B-AS1 were measured by RT-qPCR. (B) Western blotting was used to detect the expression of ZFP36. (C) The distribution of CpG islands within the ZFP36 promoter region was analyzed by the MethPrimer website. (D) MSP was adopted to detect the methylation level of the DPYD promoter region in BEAS-2B cells after CDKN2B-AS1 overexpression or silencing, and addition of DNA methyltransferase inhibitor 5-Aza-CdR (U, unmethylation; M, methylation; 5-Aza-CdR, 5-Aza-2'-deoxycytidine). (E) ChIP was employed to detect the

enrichment of DNMT1 within the ZFP36 promoter region in BEAS-2B cells after CDKN2B-AS1 overexpression. (F) RIP verified the results of CDKN2B-AS1 binding to DNMT1. Data were presented as mean ± SD. **P<0.01.

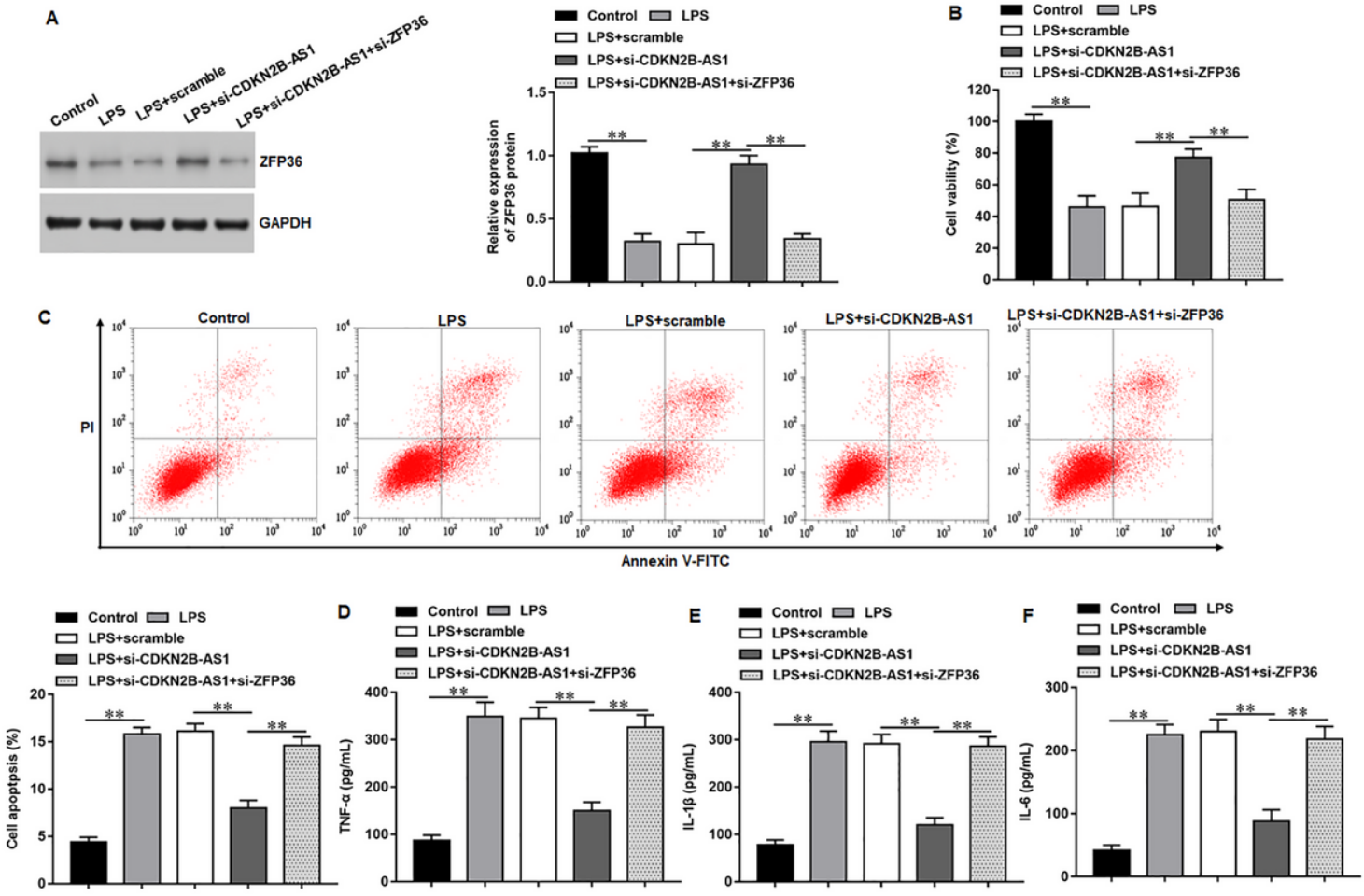

Figure 4

CDKN2B-AS1 regulates BEAS-2B cell viability, apoptosis and inflammatory response by negatively regulating ZFP36 expression. si-CDKN2B-AS1 were transfected into LPS-treated BEAS-2B cells alone or together with si-ZFP36. (A) Western blotting was used to measure the expression of ZFP36 protein. (B) BEAS-2B cell viability was evaluated by using CCK-8 assay. (C) BEAS-2B cell apoptosis was detected by using flow cytometry. (D-F) ELISA was performed to measure the levels of TNF-α, IL-1β and IL-6 in cell culture supernatant. Data were presented as mean ± SD. **P<0.01.

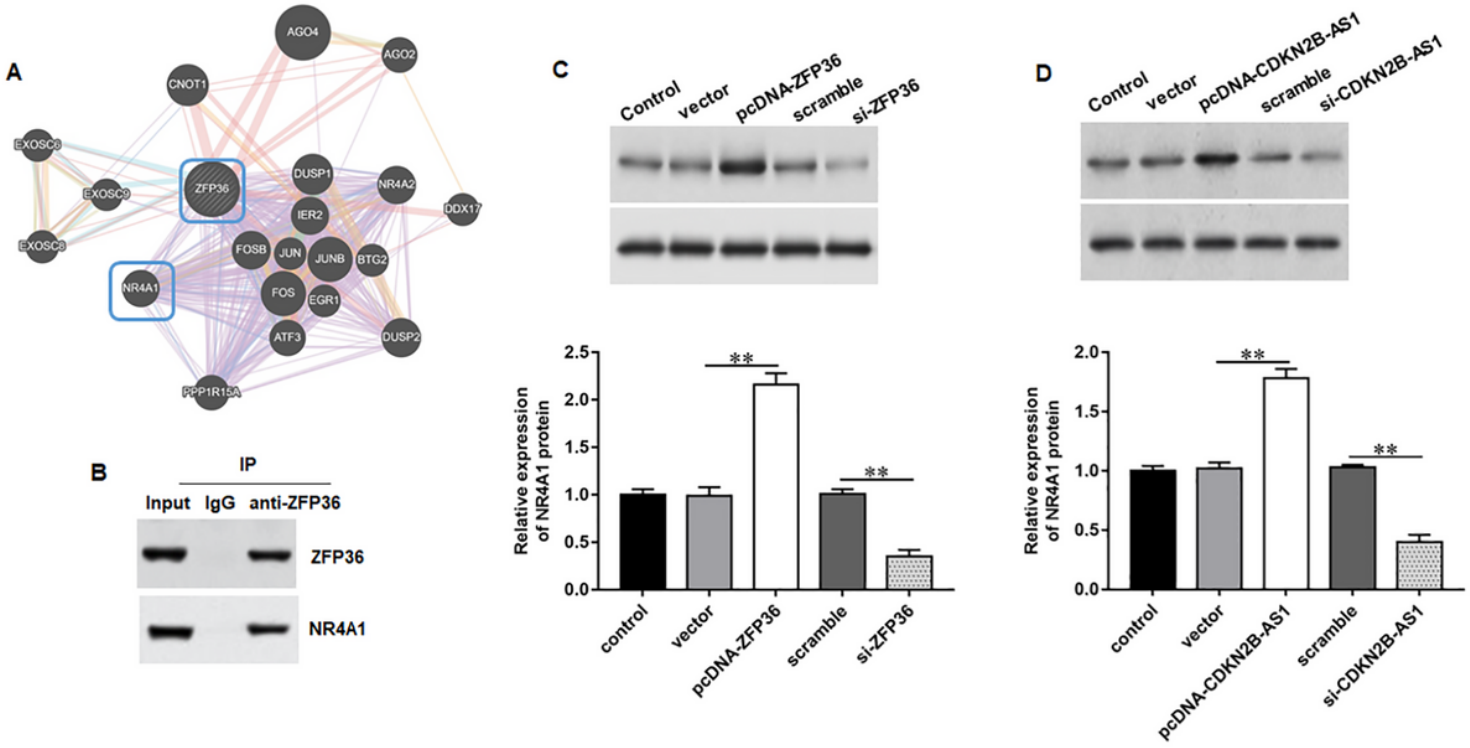

Figure 5

ZFP36 interacts with NR4A1 and positively regulates NR4A1 expression. (A) The online Genemania tool was used to predict the potential interacting proteins of ZFP36. (B) The interaction between ZFP36 protein and NR4A1 protein was verified by using Co-IP assay. (C) pcDNA-ZFP36, si-ZFP36 and their negative controls were transfected into BEAS-2B cells, respectively. Western blotting assay were used to measure NR4A1 protein expression of in BEAS-2B cells. (D) pcDNA-CDKN2B-AS1, si-CDKN2B-AS1 and their negative controls were transfected into BEAS-2B cells, respectively. Western blotting was used to detect the expression of NR4A1 protein in BEAS-2B cells. Data were presented as mean ± SD. **P<0.01.

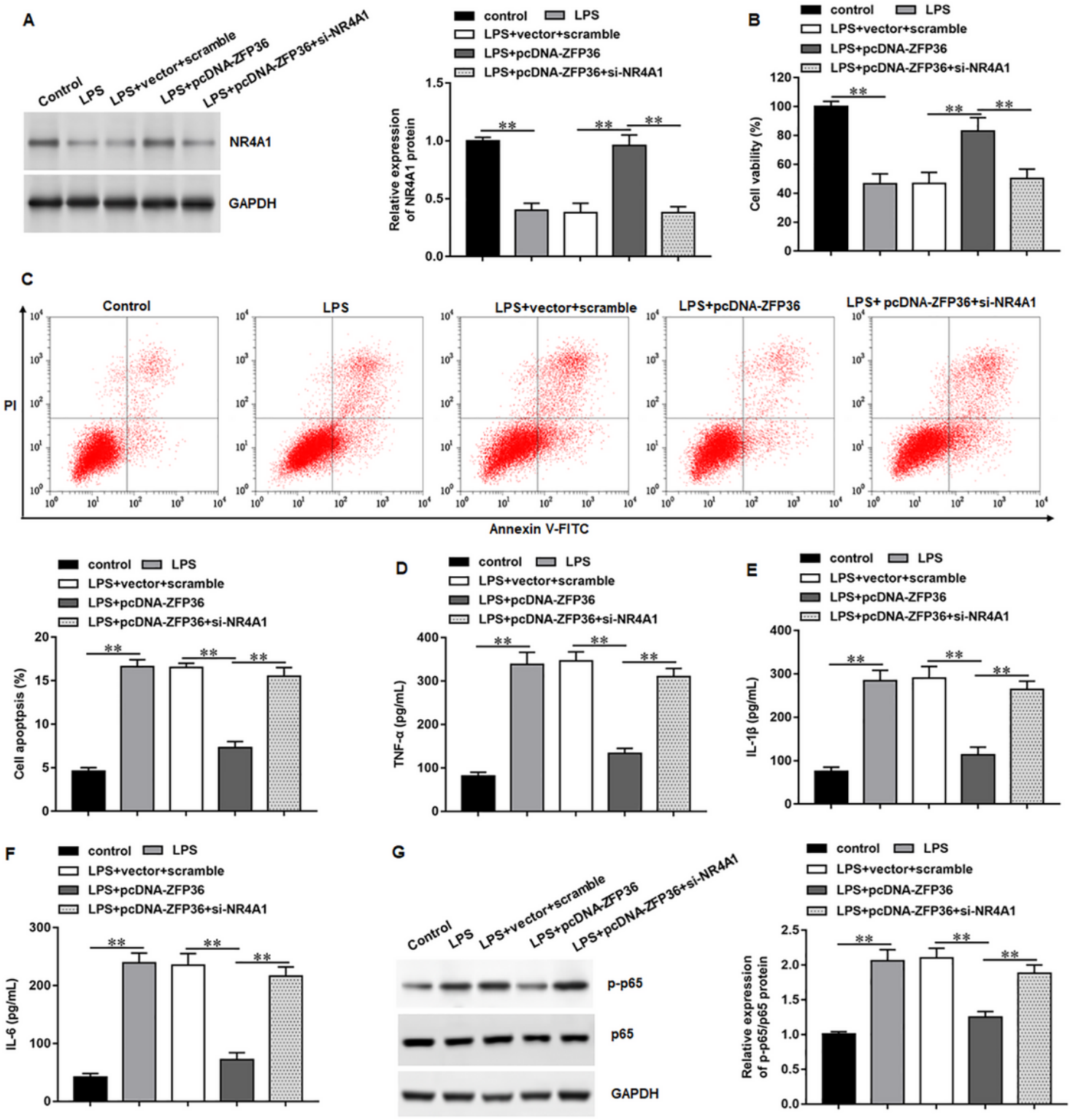

Figure 6

ZFP36 regulates BEAS-2B cell viability, apoptosis and inflammatory response by regulating NR4A1-mediated NF-κB signaling pathway pcDNA-ZFP36 were transfected into LPS-treated BEAS-2B cells alone or together with si-NR4A1 (A) Western blotting was conducted to measure the expression of NR4A1 protein. (B) CCK-8 assay was performed to evaluate BEAS-2B cell viability. (C) Flow cytometry was

performed to evaluate BEAS-2B cell apoptosis. (D-F) The levels of TNF-α, IL-1β and IL-6 in cell culture supernatant were measured by using ELISA. Data were presented as mean ± SD. **P<0.01.

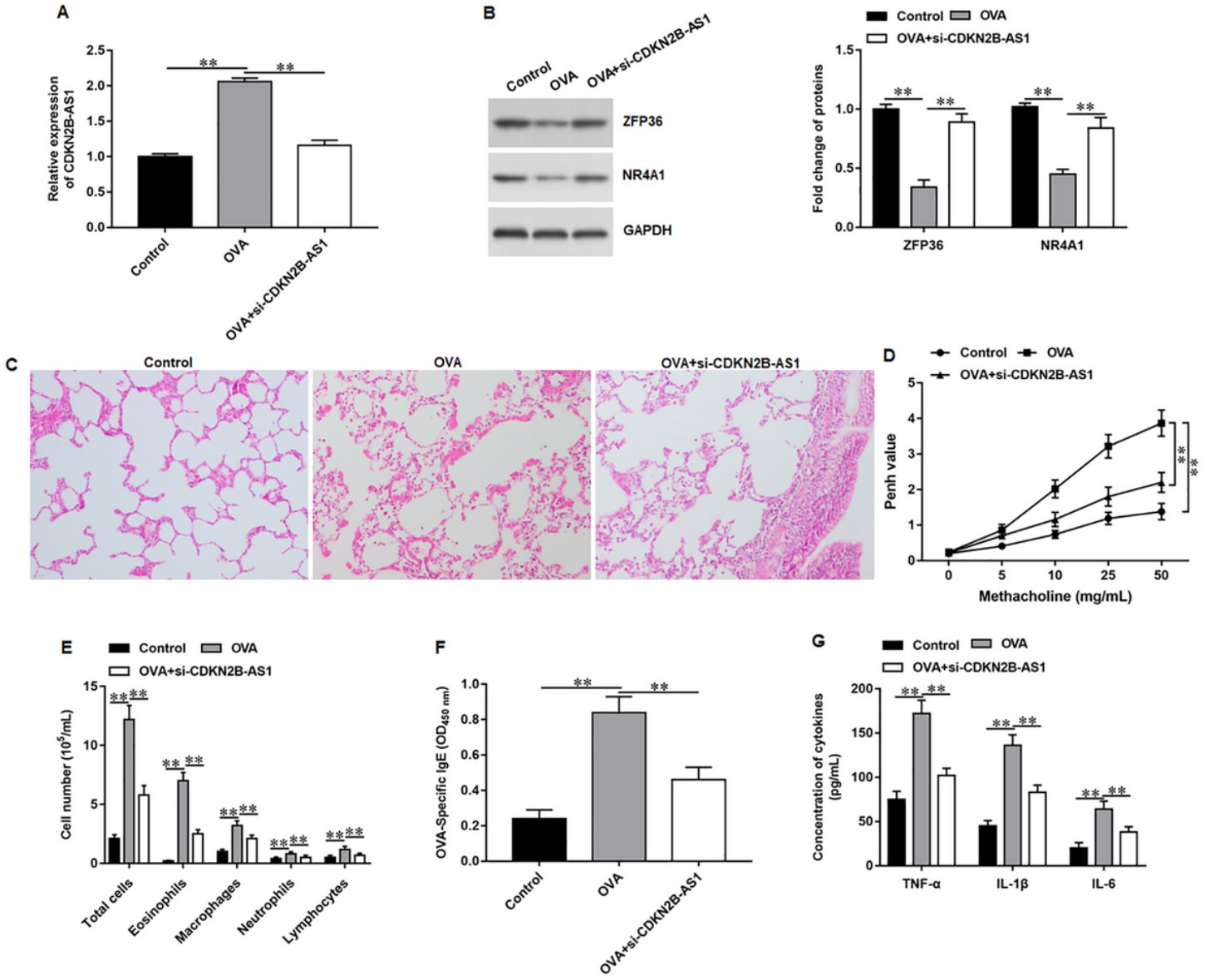

Figure 7

Silencing CDKN2B-AS1 alleviated asthma symptoms in OVA-induced asthma mice. BALB/c mice were randomly divided into three groups (n=8 per group): control group, OVA group, and OVA+si-CDKN2B-AS1 group. The mice were sensitized and challenged with OVA by intraperitoneal injection to establish asthma model, and si-CDKN2B-AS1 was intraperitoneally injected for treatment. (A) The expression of CDKNAB-AS1 in lung tissues of mice was measured by using RT-qPCR. (B) The expression of ZFP36 and NR4A1 in lung tissues of mice was detected by using Western blotting. (C) The airway hyperresponsiveness of mice in all groups was detected through measuring the Penh value. (D) Lung tissue sections from each experimental group were processed for histological evaluation, and lung inflammation was determined by observation of lung tissue sections stained with H&E staining under light microscopy. (E) Total and differential inflammatory cell count in the BALF of mice in all groups. (F) The serum OVA-specific IgE

levels of mice in all groups were detected by using ELISA. (G) The levels of TNF-α, IL-1β and IL-6 in BALF were examined by using ELISA. Data were presented as mean ± SD. **P<0.01.